

# Polyakov loop fluctuations in SU(3) lattice gauge theory and an effective gluon potential

Pok Man Lo,<sup>1</sup> Bengt Friman,<sup>1</sup> Olaf Kaczmarek,<sup>2</sup> Krzysztof Redlich,<sup>3,4</sup> and Chihiro Sasaki<sup>5</sup>

<sup>1</sup>*GSI, Helmholtzzentrum für Schwerionenforschung, Planckstrasse 1, D-64291 Darmstadt, Germany*

<sup>2</sup>*Fakultät für Physik, Universität Bielefeld, 33615 Bielefeld, Germany*

<sup>3</sup>*Institute of Theoretical Physics, University of Wrocław, PL-50204 Wrocław, Poland*

<sup>4</sup>*Extreme Matter Institute EMMI, GSI, Planckstrasse 1, D-64291 Darmstadt, Germany*

<sup>5</sup>*Frankfurt Institute for Advanced Studies, D-60438 Frankfurt am Main, Germany*

(Dated: December 31, 2017)

We calculate the Polyakov loop susceptibilities in the SU(3) lattice gauge theory using the Symanzik improved gauge action on different-sized lattices. The longitudinal and transverse fluctuations of the Polyakov loop, as well as, that of its absolute value are considered. We analyze their properties in relation to the confinement-deconfinement phase transition.

We also present results based on simulations of (2+1)-flavor QCD on  $32^3 \times 8$  lattice using Highly Improved Staggered Quark (HISQ) action by the HotQCD collaboration. The influences of fermions on the Polyakov loop fluctuations are discussed. We show, that ratios of different susceptibilities of the Polyakov loop are sensitive probes for critical behavior. We formulate an effective model for the Polyakov loop potential and constrain its parameters from existing quenched lattice data including fluctuations. We emphasize the role of fluctuations to fully explore the thermodynamics of pure gauge theory within an effective approach.

PACS numbers: 25.75.Nq, 11.15.Ha, 24.60.-k, 05.70.Jk

## I. INTRODUCTION

Lattice gauge theory provides a powerful nonperturbative approach to study the phase structure and thermodynamics of a non-abelian gauge theory.

Presumably, the best explored till now are pure lattice gauge theories with the SU(2) and SU(3) color groups [1–6]. Recently, the equation of state of the SU(3) gauge theory was established with an unprecedented precision in a broad parameter range within lattice approach [7]. The results were extrapolated to the continuum and thermodynamic limit, providing definitive results on the equation of state and the value of critical temperature.

The phase transition in the SU(3) gauge theory is first order and is characterized by the spontaneous breaking of the global  $\mathcal{Z}_3$  center symmetry of the Yang-Mills Lagrangian. The Polyakov loop is an order parameter which is linked to the free energy of the static quark immersed in a hot gluonic medium [8, 11]. At low temperatures the thermal expectation value of the Polyakov loop  $\langle |L| \rangle$  vanishes, indicating color confinement. At high temperatures  $\langle |L| \rangle \neq 0$ , resulting in the finite energy of a static quark, and consequently deconfinement of color and the spontaneous breaking of  $\mathcal{Z}_3$  center symmetry. The transition temperature can be identified from the peak position of the Polyakov loop susceptibility.

On the lattice, the ultraviolet divergence of the bare quark-antiquark free energy implies, that in the continuum limit, the bare Polyakov loop vanishes for all temperatures. Thus, the Polyakov loop and the related susceptibilities require renormalization to become physically meaningful [11, 12]. While the basic thermodynamics functions of the SU(3) pure gauge theory are well established within lattice approach, the situation is less

clear for the temperature dependence of the renormalized Polyakov loop and its susceptibilities.

In this paper we focus on the renormalized Polyakov loop susceptibilities. For color gauge group  $SU(N_c \geq 3)$ , the Polyakov loop is complex-valued. Consequently, discussing the Polyakov loop fluctuations one can consider susceptibilities along longitudinal and transverse direction, as well as, that of its absolute value.<sup>1</sup>

We calculate the temperature dependence of the Polyakov loop susceptibilities within the SU(3) lattice gauge theory. We use the Symanzik improved gauge action on  $N_\sigma^3 \times N_\tau$  lattices for different values of the temporal lattice sizes  $N_\tau = (4, 6, 8)$  and for spatial extensions  $N_\sigma$  varying from 16 to 64.

In our recent studies [13], we have discussed the ratios of different susceptibilities of the Polyakov loop and motivate their importance as observables to probe deconfinement transition in the SU(3) pure gauge theory. We have shown, that the ratios of susceptibilities display a jump across the critical temperature.

In this paper we extend our previous study and discuss properties of the Polyakov susceptibilities in a broader temperature range. We also study the influence of dynamical quarks on different susceptibilities within lattice gauge theory. We present results based on the Polyakov loop data from simulations in (2+1)-flavor QCD on  $32^3 \times 8$  lattice using the HISQ action with an almost

<sup>1</sup> In the real sector of the Polyakov loop, longitudinal and transverse components correspond to the real and imaginary direction respectively. Although the thermal average of the imaginary part of the Polyakov loop vanishes, its fluctuation along the imaginary direction does not.

physical strange quark mass and  $m_{u,d} = m_s/20$  [14, 15].

We show, that the explicit breaking of the  $\mathcal{Z}_3$  center symmetry in QCD, modifies the properties of the Polyakov loop susceptibilities found in the pure gauge theory. The ratios are substantially smoothened but still feature interesting characteristics in connection to the deconfinement phase transition.

In the confined phase and up to near  $T_c$ , the thermodynamics of the SU(3) gauge theory is well described within the Hagedorn-type model, incorporating glueballs as degrees of freedom [7]. In the deconfined phase, the perturbative approach describes the lattice data from the Stefan-Boltzmann limit down to  $T > (2 - 3)T_c$  [7]. To quantify the equation of state near  $T_c$  one needs in general, an intrinsic non-perturbative description in terms of effective models.

The Polyakov loop is the relevant quantity to effectively describe gluodynamics [16–18]. Various models based on the Polyakov loop have been proposed to quantify the deconfinement transition and thermodynamics of a pure gauge theory [16–25]

We take advantage of our new data on different susceptibilities to construct an effective potential for the Polyakov loop, which is consistent with all existing lattice data over a broad range of temperatures. We show, that the incorporation of fluctuation effects, is important to describe thermodynamics of a pure gauge theory.

The paper is organized as follows. In the next Section, we present our lattice results for the Polyakov loop susceptibilities and their ratios. In Section III we introduce the effective Polyakov loop model and its comparison with lattice data. In the last section we present our summary and conclusions.

## II. THE POLYAKOV LOOP SUSCEPTIBILITIES ON THE LATTICE

On a  $N_\sigma^3 \times N_\tau$  lattice, the Polyakov loop is defined as the trace of the product over temporal gauge links,

$$L_{\vec{x}}^{\text{bare}} = \frac{1}{N_c} \text{Tr} \prod_{\tau=1}^{N_\tau} U(\vec{x}, \tau), \quad (1)$$

$$L^{\text{bare}} = \frac{1}{N_\sigma^3} \sum_{\vec{x}} L_{\vec{x}}^{\text{bare}}. \quad (2)$$

Due to the  $\mathcal{Z}_3$  symmetry of the pure gauge action, this quantity is exactly zero, when averaging over all gauge field configurations. Furthermore, the Polyakov loop is strongly  $N_\tau$  dependent and needs to be renormalized. We consider the multiplicatively renormalized Polyakov loop [11],

$$L^{\text{ren}} = (Z(g^2))^{N_\tau} L^{\text{bare}} \quad (3)$$

and introduce the ensemble average of the modulus thereof,  $\langle |L^{\text{ren}}| \rangle$ . The latter is well defined in the continuum and thermodynamic limits.

The thermal average of the renormalized Polyakov loop can also be obtained from the long distance behavior of the renormalized heavy quark-antiquark free energy  $F_{q\bar{q}}^{\text{ren}}$  [11], which is defined by the correlation function

$$\langle L_{\vec{x}}^{\text{ren}} L_{\vec{y}}^{\text{ren} \dagger} \rangle = e^{-F_{q\bar{q}}^{\text{ren}}(r=|\vec{x}-\vec{y}|, T)/T} \quad (4)$$

$$r \rightarrow \infty \quad |\langle L^{\text{ren}} \rangle|^2.$$

In the confined phase, the heavy quark-antiquark free energy rises linearly with distance as  $r \rightarrow \infty$ , hence the Polyakov loop vanishes. The Polyakov loop is finite in the deconfined phase, and can serve as an order parameter for the spontaneous breaking of the  $\mathcal{Z}_3$  center symmetry. Note that both definitions, (3) and (4), are equivalent in the thermodynamic limit.

Using the renormalized Polyakov loop, one can define the renormalized Polyakov loop susceptibility as

$$T^3 \chi_A = \frac{N_\sigma^3}{N_\tau^3} (\langle |L^{\text{ren}}|^2 \rangle - \langle |L^{\text{ren}}| \rangle^2). \quad (5)$$

Here, we anticipate the factor  $T^3$  to define (5) as an observable in the continuum limit.

In the SU(3) gauge theory, the Polyakov loop operator is complex. Thus in addition to  $\chi_A$ , one can also explore the longitudinal and transverse fluctuations of the Polyakov loop [13]

$$T^3 \chi_L = \frac{N_\sigma^3}{N_\tau^3} [\langle (L_L^{\text{ren}})^2 \rangle - \langle L_L^{\text{ren}} \rangle^2]. \quad (6)$$

$$T^3 \chi_T = \frac{N_\sigma^3}{N_\tau^3} [\langle (L_T^{\text{ren}})^2 \rangle - \langle L_T^{\text{ren}} \rangle^2], \quad (7)$$

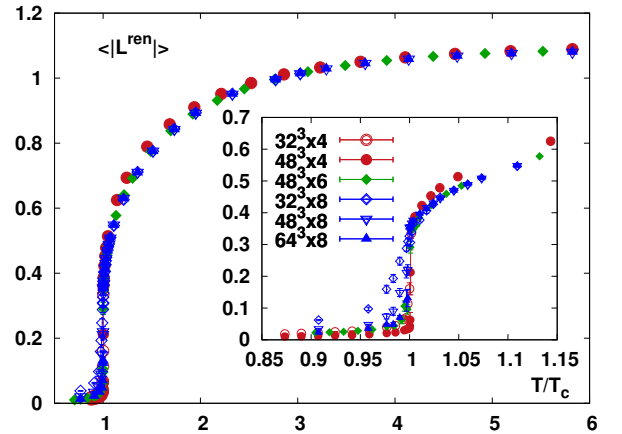


FIG. 1: The temperature dependence of the modulus of the renormalized Polyakov loop in the SU(3) gauge theory, calculated on various lattices.

We have computed the Polyakov loop susceptibilities using the (1,2)-tree-level Symanzik improved gauge action on a  $N_\sigma^3 \times N_\tau$  lattice. We consider lattices of temporal size  $N_\tau = 4, 6$  and 8 and spatial extent  $N_\sigma$  varying

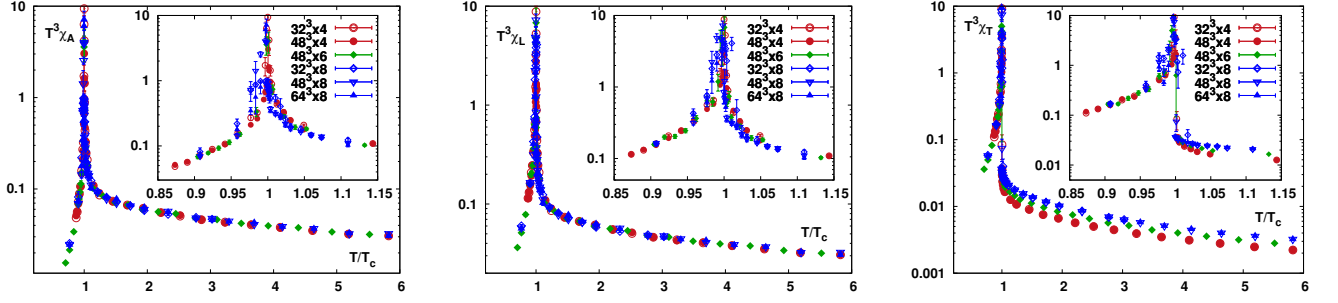


FIG. 2: The temperature dependence of the renormalized Polyakov loop susceptibilities from Eqs. (5), (6) and (7), calculated on various lattice sizes, in the SU(3) pure gauge theory. The temperature is normalized to its critical value.

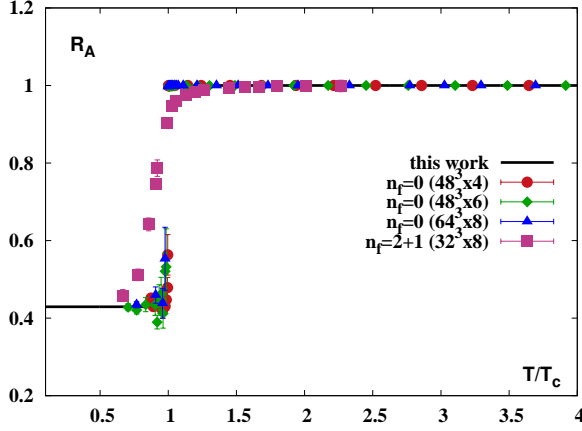


FIG. 3: The ratio of the absolute (5) to longitudinal (6) part of the Polyakov loop susceptibilities calculated within lattice gauge theory for pure gauge system and (2+1)-flavor QCD (see text). The temperature is normalized to its (pseudo) critical value for respective lattice. The line is the model result explained in the text.

from 16 to 64. The temperatures for the three temporal lattice extents are set by varying the bare coupling and use the temperature scale determined by the zero temperature string tension, as well as the critical couplings of the deconfinement transition [9, 10]. The gauge field configurations were generated using one heatbath and four overrelaxation updates per sweep with 15 000 sweeps in general and up to 100 000 sweeps close to the critical temperature,  $T_c$ .

The renormalization constants,  $Z(g^2)$ , were taken from [11]. The statistical errors were obtained from a Jackknife analysis and do not include any systematic error resulting from the renormalization procedure. In Fig. 1, we show the lattice gauge theory result for  $\langle |L^{\text{ren}}| \rangle$  as a function of temperature.

While no volume effects are visible in the deconfined phase, data at fixed  $N_\tau$  in the confined phase, show the expected  $1/\sqrt{V}$  volume-dependence. Considering results at fixed ratio  $N_\sigma/N_\tau$ , only small cut-off effects can be observed at high as well as at low temperatures. The

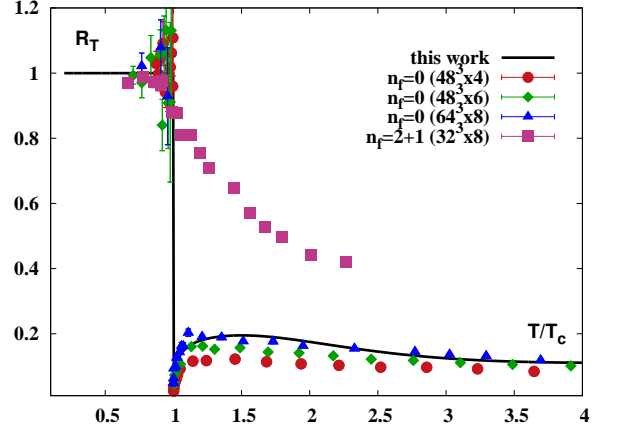


FIG. 4: Lattice results on the ratio of the transverse (7) to longitudinal (6) susceptibility of the Polyakov loop for pure gauge system and (2+1)-flavor QCD. The line is the Polyakov loop model result discussed in Section III.

deviation of the  $N_\tau = 4$  and 8 data between  $(1-2)T_c$  may be attributed to the uncertainty in the determination of the renormalization constants, rather than to the cut-off effects.

The results for the renormalized Polyakov loop susceptibilities obtained on different lattice sizes are shown in Fig. 2. In the close vicinity of the phase transition,  $0.95 < T/T_c < 1.05$ , all three susceptibilities show rather strong cut-off and volume effects. Such behavior is expected due to the first order nature of the phase transition in pure gauge theory. Outside this region, the fluctuations of longitudinal and the modulus of the Polyakov loop, show only minimal dependence on  $N_\tau$  and  $N_\sigma$  in both phases. The transverse susceptibility  $\chi_T$  in Fig. 2, however, is seen to exhibit stronger  $N_\tau$  dependence in the deconfined phase.

### A. The ratios of susceptibilities

The ambiguities from the renormalization scheme can be avoided by considering the ratios of the susceptibilities

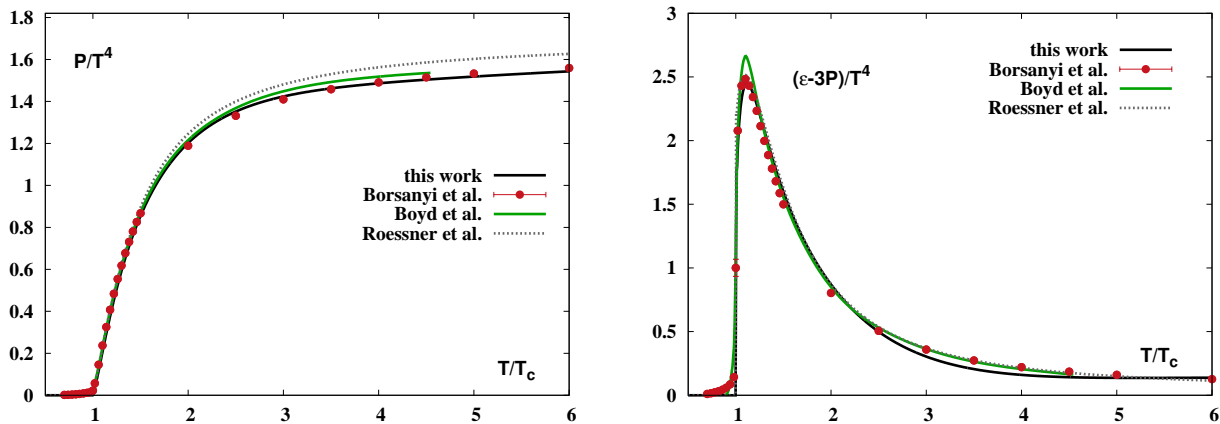


FIG. 5: Left-hand figure: Lattice QCD data for thermodynamic pressure obtained in the SU(3) gauge theory. The points are from Ref. [7], whereas the green line is the parametrization of lattice data from Ref. [5]. The black and the dashed lines are obtained in the Polyakov loop models introduced in Section III. Right-hand figure: As in the left-hand figure but for the interaction measure  $(\epsilon - 3P)/T^4$ , where  $\epsilon$  is the energy density.

of the Polyakov loop. These are particularly interesting observables to identify the deconfinement phase transition [13]. In the following, we study the influences of dynamical quarks on these ratios.

Figs. 3 and 4 show the ratios  $R_A = \chi_A/\chi_L$  and  $R_T = \chi_T/\chi_L$  of different susceptibilities obtained in the SU(3) pure gauge theory. Also shown in this figure are results obtained in lattice QCD with (2+1)-flavor HISQ action and for almost physical quark masses. For  $N_f \neq 0$ , the temperature in Figs. 3 and 4 is normalized to the corresponding pseudo critical temperature at fixed number of flavors [14, 15].

In the SU(3) pure gauge theory ( $N_f = 0$ ), the ratios  $R_A$  and  $R_T$  exhibit a  $\theta$ -like discontinuity at  $T_c$ , and change only weakly with temperature on either side of the transition. Consequently, the ratios of the Polyakov loop susceptibilities, can be considered as an excellent probe of the phase change. In the confined phase, their constant values can be deduced from general symmetry arguments, and the observation that these susceptibilities are dominated by the quadratic terms of the effective action [13]. In the deconfined phase, the ratio  $R_A \simeq 1$ , as long as, the center symmetry is spontaneously broken in the real sector. The properties of  $R_T$  above  $T_c$  seen in Fig. 4 indicate, that in the SU(3) pure gauge theory the fluctuations of the longitudinal part of the Polyakov loop exceed that of the transverse part, while keeping the ratio almost  $T$ -independent.

In the presence of dynamical quarks, the Polyakov loop is no longer an order parameter and stays finite even in the low temperature phase. Consequently, the ratios of the Polyakov loop susceptibilities are modified due to explicit breaking of the  $Z_3$  center symmetry. We therefore expect the smoothening of these ratios across the pseudo critical temperature. Indeed Figs. 3 and 4 show, that in the presence of dynamical quarks, both ratios vary continuously with temperature. We observe that  $R_A$  inter-

polates between the two limiting values set by the pure gauge theory, while the width of crossover region can correlate with the number of flavors and values of their masses.

The ratio  $R_T$  is strongly influenced by the existence of quarks. In addition to the stronger smoothening effect observed, its numerical values in the deconfined phase become temperature dependent, and deviate substantially from the pure gauge result. We also note the abrupt change of slopes of  $R_T$  and  $R_A$  near their respective transition point, in spite of the fact, that the light quark masses are small.

A more quantitative investigations of the effects of quarks on the Polyakov loop susceptibilities require further studies on the system size and the quark mass dependence of these quantities, as well as their extrapolation to the continuum and thermodynamic limit. We defer such analysis to later research.

### III. THE POLYAKOV LOOP POTENTIAL

The non-perturbative aspects of QCD thermodynamics can be studied using effective models, with quarks and Polyakov loop as relevant degrees of freedom [16–25]. The parameters of such models are fixed, so as to reproduce the lattice results on different observables. We take advantage of our new lattice data on the Polyakov loop susceptibilities to construct a phenomenological Polyakov loop potential which takes fluctuations into account.

The most commonly used Polyakov loop models are the polynomial [21] and the logarithmic potential [17, 22, 23], the latter includes the contribution of SU(3) Haar measure. While both models are constructed to match the lattice data on the equation of state and the average Polyakov loop, they predict very different results for the Polyakov loop susceptibilities. In particular, the poly-

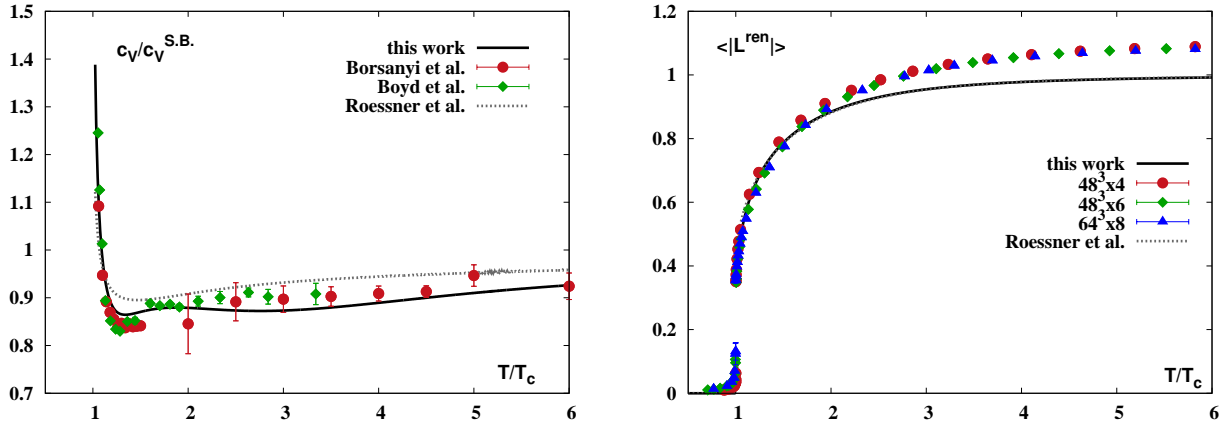


FIG. 6: Left-hand figure: The specific heat normalized to its Stefan Boltzmann limit obtained from lattice data from Refs. [5] and [7], see text. Right-hand figure: Points are the thermal averages of the renormalized Polyakov loop as in Fig. 1. The lines are the Polyakov loop model results discussed in Section III.

mial model suggests, that for  $T > T_c$ , the ratio  $R_T > 1$ , while the logarithmic model gives  $R_T < 1$ . In this regard, the lattice data in Fig. 4 clearly favors the model with the Haar measure included. Moreover, as noticed in Ref. [23], the ratio  $R_T > 1$ , would lead to the negative susceptibility  $\chi_{LL} = \chi_L - \chi_T$ , which is unphysical. This is in line with the theoretical expectation, that the logarithmic model is preferred, as it enforces the restriction of the Polyakov loop to the target region [17].

Figs. 5 and 6 show comparison of the logarithmic potential model from Ref. [22] with the SU(3) lattice data. The model provides a reasonable description of the lattice equation of state and the specific heat. However, the temperature dependence of the renormalized Polyakov loop is described only in the vicinity of  $T_c$ . This is hardly surprising, since the lattice data on the renormalized Polyakov loop overshoot unity at  $T > 3T_c$ . For any potential model, that complies to the restriction of the Haar measure, the Polyakov loop can never exceed unity. To tackle this problem in model calculations, we employ a smooth extrapolation of lattice data, from the temperature range  $(1.0 - 1.6)T_c$ , to unity at high temperature. Fig. 6-right shows such matching of the model results from Ref. [22] to the SU(3) lattice data on the renormalized Polyakov loop.

The potential from Ref. [22] fails to reproduce the temperature dependence of the longitudinal and transverse susceptibility of the Polyakov loop, as seen in Fig. 7. Thus, considerations of the equation of state and  $\langle |L| \rangle$  alone, are not sufficient to describe the pure Yang-Mills thermodynamics. One needs to take into account the effects of fluctuations.

To construct the thermodynamic potential, which is capable to quantify lattice data on fluctuations, we con-

sider the following  $\mathcal{Z}_3$  symmetric model

$$\frac{U(L, \bar{L})}{T^4} = -\frac{1}{2}a(T)\bar{L}L + b(T)\ln M_H(L, \bar{L}) + \frac{1}{2}c(T)(L^3 + \bar{L}^3) + d(T)(\bar{L}L)^2, \quad (8)$$

where  $M_H$  is the SU(3) Haar measure, which is expressed by the Polyakov loop and its conjugate, as

$$M_H = 1 - 6\bar{L}L + 4(L^3 + \bar{L}^3) - 3(\bar{L}L)^2. \quad (9)$$

The restriction of the Polyakov loop to the target region is naturally enforced by the Haar measure. For the special case of vanishing  $c(T)$  and  $d(T)$ , the potential in Eq. (8) reduces to the same form used in Ref. [22].

The potential parameters, can be uniquely determined from the lattice data on the equation of state, the Polyakov loop expectation value, as well as, its susceptibilities. The numerical values for model parameters and a description of methods applied are summarized in the Appendix II. The model predictions on different thermodynamic observables are compared with lattice data in Figs. 4-7.

Fig. 5 shows, that there is a very satisfactory description of lattice results on the thermodynamic pressure and the interaction measure, up to very high temperatures. Our model parameters are tuned to describe the most recent [7], rather than previous [5], lattice data on the thermodynamic pressure. This yields small differences between our and the previous [22] Polyakov loop model results.

The comparison of model predictions with lattice data for heat capacity  $c_V$ , normalized to its Stefan Boltzmann limit  $c_V^{\text{SB}} = (32\pi^2/15)T^3$ , is shown in Fig. 6. The lattice data for  $c_V(T)$  were extracted from the respective continuum pressure results. The derivatives were calculated by taking central differences between data points. The errors were estimated by  $\mathcal{O}[h^2]$ , where  $h = \delta T/T$  and  $\delta T$  is the difference between the grids around the specific



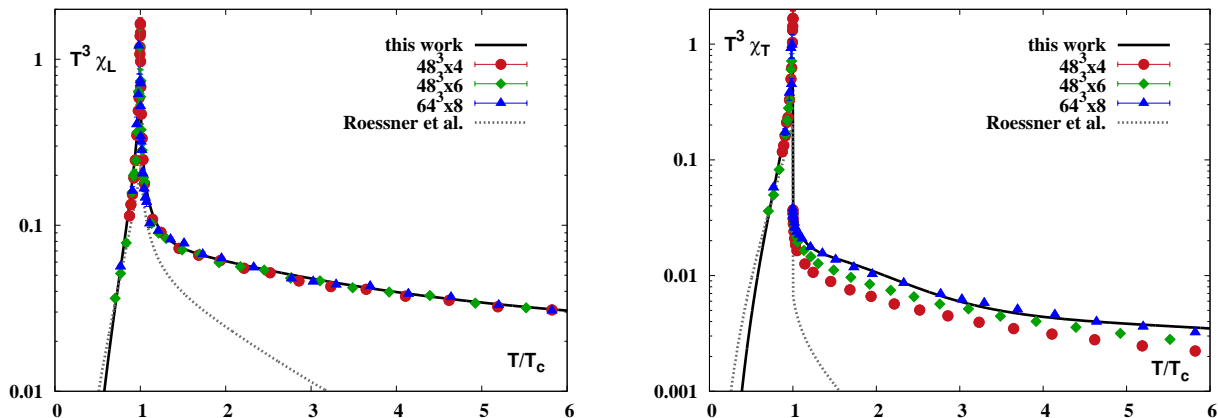


FIG. 7: Lattice data for the longitudinal (left-hand figure) and the transverse (right-hand figure) Polyakov loop fluctuations from Fig. 2. The lines are the corresponding potential model results discussed in Section III.

point. The  $c_V$  exhibits a shallow minimum above  $T_c$ , which is reproduced by the present Polyakov loop model quite satisfactory.

The essential difference between our model in Eq. (8) and the previously proposed logarithmic potential, lies in the prediction for the Polyakov loop fluctuations. Figs. 7 shows, that both the longitudinal and the transverse susceptibility are very well described by the new Polyakov loop potential, while the logarithmic model tends to underestimate both susceptibilities.

#### IV. CONCLUSIONS

We have calculated the Polyakov loop susceptibilities in the SU(3) lattice gauge theory for different number of quark flavors,  $N_f = 0$  and  $N_f = (2 + 1)$ . For (2+1)-flavor QCD, the susceptibilities were calculated from the Polyakov loop results from [15], where the HISQ action with almost physical strange quark mass and  $m_{u,d} = m_s/20$  was used. For all cases, the extrapolations to the continuum and thermodynamic limit have not been performed yet.

We have discussed the temperature dependence of the longitudinal  $\chi_L$ , the transverse  $\chi_T$  and the absolute value  $\chi_A$  of the Polyakov loop fluctuations. We have analyzed general properties of the Polyakov loop susceptibilities in relation to the color group structure and motivated their ratios,  $R_A = \chi_A/\chi_L$  and  $R_T = \chi_T/\chi_L$ , as relevant observables to probe deconfinement.

A remarkable feature of different ratios of the Polyakov loop susceptibilities is their strong sensitivity to a phase change in a system. In the SU(3) pure gauge theory the ratios of susceptibilities show discontinuity at the critical point and exhibit a very weak, but different, temperature dependence in the confined and deconfined phase. The explicit breaking of the  $Z_3$  center symmetry in QCD, due to quark fields, modifies this property.

The  $R_A$ , and in particular  $R_T$  ratios are substantially

smoothened, yet still display interesting features related to the deconfinement. The  $R_A$  converges to the asymptotic values found in a pure gauge theory, both in the confined and the deconfined phase. Whereas, the  $R_T$  converges only to the low temperature limit of a pure gauge theory. At high temperatures and for light quarks, it differs substantially from the results obtained in a pure gauge theory.

We have used our data on the Polyakov loop susceptibilities to construct an effective Polyakov loop potential, which is consistent with all lattice results over a broad range of temperatures. We have shown, that the incorporation of fluctuations is important to describe thermodynamics of a pure gauge theory within the effective approach. The Polyakov loop potential developed in this work is open to a more realistic effective description of QCD thermodynamics with quarks.

#### Acknowledgments

We acknowledge stimulating discussions with Jürgen Engels, Frithjof Karsch and Helmut Satz. We are grateful to Peter Petreczky, Alexei Bazavov and the HotQCD Collaboration for providing us with data for the Polyakov loop. P.M.L. acknowledges the support of the Frankfurt Institute for Advanced Studies (FIAS). B.F. is supported in part by the Extreme Matter Institute EMMI. K.R. acknowledges partial support of the Polish Ministry of National Education (NCN). The work of C.S. has been partly supported by the Hessian LOEWE initiative through the Helmholtz International Center for FAIR (HIC for FAIR). The numerical calculations have been performed on the Bielefeld GPU Cluster.

$T/T_c$	$\langle  L^{\text{ren}}  \rangle$	$T^3\chi_A$	$T^3\chi_L$	$T^3\chi_T$
0.768	0.0132(1)	0.0245(4)	0.0564(12)	0.0576(16)
0.908	0.0225(6)	0.074(4)	0.161(10)	0.174(11)
0.958	0.0349(17)	0.178(24)	0.405(44)	0.379(53)
0.977	0.0478(36)	0.344(42)	0.615(86)	0.92(17)
0.983	0.0484(62)	0.56(25)	1.21(39)	0.450(53)
0.990	0.0699(62)	0.79(16)	2.14(47)	0.99(23)
0.997	0.124(34)	6.(2)	4.40(85)	10.(3)
0.998	0.132(27)	7.(2)	12.(4)	4.(1)
1.000	0.354(8)	0.74(16)	0.75(16)	0.038(2)
1.001	0.357(5)	0.71(10)	0.71(10)	0.035(1)
1.002	0.367(3)	0.520(65)	0.521(65)	0.033(1)
1.004	0.374(3)	0.343(20)	0.343(20)	0.032(1)
1.010	0.398(3)	0.319(28)	0.319(28)	0.0305(6)
1.017	0.412(2)	0.283(30)	0.283(30)	0.0286(6)
1.024	0.432(2)	0.207(13)	0.207(13)	0.0263(4)
1.031	0.446(1)	0.204(12)	0.204(12)	0.0257(3)
1.045	0.469(1)	0.166(7)	0.166(7)	0.0239(2)
1.059	0.490(1)	0.147(10)	0.147(10)	0.0239(4)
1.073	0.509(1)	0.138(8)	0.138(8)	0.0224(3)
1.109	0.548(1)	0.102(5)	0.102(5)	0.0209(3)
1.211	0.630(1)	0.092(3)	0.092(3)	0.0176(2)
1.354	0.709(1)	0.082(2)	0.082(2)	0.0155(2)
1.512	0.775(0)	0.078(2)	0.078(2)	0.0137(2)
1.731	0.842(0)	0.067(2)	0.067(2)	0.0118(2)
1.951	0.892(0)	0.063(2)	0.063(2)	0.0103(1)
2.328	0.951(0)	0.056(1)	0.056(1)	0.0086(1)
2.772	0.995(0)	0.048(1)	0.048(1)	0.00692(1)
3.026	1.014(0)	0.046(1)	0.046(1)	0.00622(1)
3.294	1.029(0)	0.044(1)	0.044(1)	0.00578(1)
3.694	1.045(0)	0.043(1)	0.043(1)	0.00509(1)
4.140	1.058(0)	0.039(1)	0.039(1)	0.00458(0)
4.639	1.068(0)	0.037(1)	0.037(1)	0.00399(1)
5.198	1.076(0)	0.033(1)	0.033(1)	0.00361(0)
5.823	1.081(0)	0.031(1)	0.031(1)	0.00322(0)

TABLE I: The lattice results for the Polyakov loop and its susceptibilities, defined in Eqs. (5)–(7), obtained in the SU(3) pure gauge theory on  $64^3 \times 8$  lattice.

### Appendix I

In Table I, we summarize our lattice results on the Polyakov loop and its susceptibilities for SU(3) pure gauge theory on  $64^3 \times 8$  lattice.

### Appendix II

To fix parameters of the phenomenological gluon potential introduced in Eq. (8), we first express  $U(L, \bar{L})$  in

terms of longitudinal  $L_L$  and transverse  $L_T$  parts of the Polyakov loop,

$$\frac{U(L_L, L_T)}{T^4} = -\frac{a(T)}{2}(L_L^2 + L_T^2) + b(T) \ln M_H \quad (10)$$

$$+ c(T)(L_L^3 - 3L_L L_T^2) + d(T)(L_L^2 + L_T^2)^2$$

with the Haar measure,

$$M_H = 1 - 6(L_L^2 + L_T^2) + 8(L_L^3 - 3L_L L_T^2) - 3(L_L^2 + L_T^2)^2, \quad (11)$$

and the parameters  $a(T)$ ,  $b(T)$ ,  $c(T)$  and  $d(T)$ .

The expectation values of both components of the Polyakov loop are obtained by solving the gap equations,

$$\frac{\partial U(L_L, L_T)}{\partial L_L} = 0, \quad \frac{\partial U(L_L, L_T)}{\partial L_T} = 0. \quad (12)$$

Focusing on the real sector, we denote the solutions of the gap equations as,  $L_T = 0$  and  $L_L = L_0$ . The pressure is then given by

$$\frac{P}{T^4} = -\frac{U}{T^4}(L_L \rightarrow L_0, L_T \rightarrow 0; T). \quad (13)$$

To calculate the susceptibilities, we construct the curvature tensor,

$$\hat{C}_{ik} = \frac{1}{T^4} \frac{\delta^2 U}{\delta L_i \delta L_k}, \quad (14)$$

which is a  $2 \times 2$  matrix, with  $L_k = \{L_L, L_T\}$ . The susceptibility matrix is defined as,  $T^3 \hat{\chi} = \hat{C}^{-1}$ .

In the real sector, the susceptibility matrix is diagonal. The explicit expressions for the longitudinal and transverse Polyakov loop susceptibilities read

$$(T^3 \chi_L)^{-1} = -a(T) + b(T) \left( -\frac{3}{(L_0 - 1)^2} - \frac{9}{(1 + 3L_0)^2} \right) + 6L_0 c(T) + 12d(T)L_0^2, \quad (15)$$

$$(T^3 \chi_T)^{-1} = -a(T) + b(T) \frac{12(1 + L_0(4 + L_0))}{(L_0 - 1)^3(1 + 3L_0)} - 6L_0 c(T) + 4d(T)L_0^2. \quad (16)$$

These two expressions, together with the gap and pressure equations, are sufficient to determine the potential parameters at different temperatures, having the lattice data for the thermodynamics observables.

The unique matching of model parameters with lattice data is only possible in the symmetry broken phase. In the confined phase, the Polyakov loop vanishes and the set of equations is no longer linear independent. The lattice susceptibilities data constrain only the quadratic terms in the effective potential and there is no restriction on parameters  $c(T)$  and  $d(T)$ . In principle, they can be

$a_1$	$a_2$	$a_3$	$a_4$	$a_5$
-44.14	151.4	-90.0677	2.77173	3.56403
$b_1$	$b_2$	$b_3$	$b_4$	
-0.32665	-82.9823	3.0	5.85559	
$c_1$	$c_2$	$c_3$	$c_4$	$c_5$
-50.7961	114.038	-89.4596	3.08718	6.72812
$d_1$	$d_2$	$d_3$	$d_4$	$d_5$
27.0885	-56.0859	71.2225	2.9715	6.61433

TABLE II: The numerical values of the parameters  $a(T)$ ,  $b(T)$ ,  $c(T)$  and  $d(T)$  for the Polyakov loop potential in Eq. (8), under the parametrizations introduced in Eqs. (17) and (18).

fixed by lattice data on higher order cumulants of the Polyakov loops, which are neglected in the present study.

The temperature dependence of model parameters in Eq. (10) can be expressed by the following parametrizations,

$$x(T) = (x_1 + x_2/t + x_3/t^2)(1 + x_4/t + x_5/t^2)^{-1} \quad (17)$$

for  $x = (a, c, d)$ , whereas  $b(T)$  is parameterized as

$$b(T) = b_1 t^{-b_4} (1 - e^{b_2/t^{b_3}}), \quad (18)$$

where  $t = T/T_c$  and  $T_c$  is the deconfinement temperature in the SU(3) lattice gauge theory.

Table II summarizes our numerical results for the model parameters. The model potential is constructed to quantitatively describe SU(3) lattice data of different thermodynamic observables, including results for the Polyakov loop susceptibilities.

We have employed lattice results for thermodynamic pressure and interaction measure from Ref. [7], while the results for the Polyakov loop were taken from Ref. [11]. The data for the longitudinal and transverse Polyakov loop susceptibilities, incorporated into our effective potential, were introduced in Section II.

Currently, the lattice data on the Polyakov loop susceptibilities are available only in the temperature interval  $0.8 < T/T_c < 6$ . Our model parameters, presented in Table II, are inherently restricted to this range.

- 
- [1] J. Engels, J. Fingberg, and M. Weber, Nucl. Phys. B **332** (1990) 737.
- [2] J. Engels, J. Fingberg, F. Karsch, D. Miller, and M. Weber, Phys. Lett. B **252** (1990) 625.
- [3] J. Engels, F. Karsch, and K. Redlich, Nucl. Phys. B **435** (1995) 295.
- [4] J. Engels and T. Scheideler, Nucl. Phys. B **539** (1999) 557.
- [5] G. Boyd, J. Engels, F. Karsch, E. Laermann, C. Legeland, M. Lutgemeier, and B. Petersson, Phys. Rev. Lett. **75** (1995) 4169.
- [6] G. Boyd, J. Engels, F. Karsch, E. Laermann, C. Legeland, M. Lutgemeier, and B. Petersson, Nucl. Phys. B **469** (1996) 419.
- [7] S. Borsanyi, G. Endrodi, Z. Fodor, S. D. Katz, and K. K. Szabo, JHEP **1207** (2012) 056.
- [8] L. D. McLerran and B. Svetitsky, Phys. Lett. B **98** (1981) 195. L. D. McLerran and B. Svetitsky, Phys. Rev. D **24** (1981) 450.
- [9] R. G. Edwards, U. M. Heller, and T. R. Klassen, Nucl. Phys. B **517** (1998) 377.
- [10] B. Beinlich, F. Karsch, E. Laermann, and A. Peikert, Eur. Phys. J. C **6** (1999) 133.
- [11] O. Kaczmarek, F. Karsch, P. Petreczky, and F. Zantow, Phys. Lett. B **543** (2002) 41.
- [12] U. M. Heller and F. Karsch, Nucl. Phys. B **251** (1985) 254. R. V. Gavai, Phys. Lett. B **691** (2010) 146. S. Gupta, K. Huebner, and O. Kaczmarek, Phys. Rev. D **77** (2008) 034503.
- [13] P. M. Lo, B. Friman, O. Kaczmarek, K. Redlich, and C. Sasaki, Phys. Rev. D **88** (2013) 014506.
- [14] M. Cheng, N. H. Christ, S. Datta, J. van der Heide, C. Jung, F. Karsch, O. Kaczmarek, and E. Laermann *et al.*, Phys. Rev. D **77** (2008) 014511. A. Bazavov, T. Bhattacharya, M. Cheng, N. H. Christ, C. DeTar, S. Ejiri, S. Gottlieb, and R. Gupta *et al.*, Phys. Rev. D **80** (2009) 014504.
- [15] A. Bazavov, T. Bhattacharya, M. Cheng, C. DeTar, H. T. Ding, S. Gottlieb, R. Gupta and P. Hegde *et al.*, Phys. Rev. D **85**, 054503 (2012).
- [16] P. N. Meisinger, T. R. Miller, and M. C. Ogilvie, Phys. Rev. D **65** (2002) 034009.
- [17] K. Fukushima, Phys. Lett. B **591** (2004) 277.
- [18] C. Sasaki and K. Redlich, Phys. Rev. D **86** (2012) 014007.
- [19] A. Dumitru, Y. Hatta, J. Lenaghan, K. Orginos, and R. D. Pisarski, Phys. Rev. D **70** (2004) 034511.
- [20] A. Dumitru and R. D. Pisarski, Phys. Rev. D **66** (2002) 096003.
- [21] C. Ratti, M. A. Thaler, and W. Weise, Phys. Rev. D **73** (2006) 014019.
- [22] S. Roessner, C. Ratti, and W. Weise, Phys. Rev. D **75** (2007) 034007.
- [23] C. Sasaki, B. Friman, and K. Redlich, Phys. Rev. D **75** (2007) 074013.
- [24] T. K. Herbst, J. M. Pawłowski, and B. -J. Schaefer, Phys. Lett. B **696** (2011) 58. T. K. Herbst, J. M. Pawłowski, and B. -J. Schaefer, arXiv:1302.1426 [hep-ph].
- [25] K. Fukushima and C. Sasaki, Progress in Particle and Nuclear Physics **72** (2013) 99.